SOME COMMENTS ON PBL PARAMETERIZATIONS IN WRF

Mariusz Pagowski *
NOAA Research – Forecast System Laboratory

1. INTRODUCTION

The Weather Research and Forecasting (WRF) model currently offers three options for parameterization of turbulence in the boundary-layer (BL hereafter): Eta implementation of 1.5-order closure of Mellor and Yamada (1982) by Janjić (1994) (MYJ), the Medium-Range Forecast (MRF) scheme based on Troen and Mahrt (1986) and Hong and Pan (1996) and the Yonsei University (YSU) scheme (Hong and Dudhia 2003), which is a modification of the MRF scheme to include explicit entrainment fluxes of heat, moisture and momentum, counter-gradient transport of momentum, and different specification of the BL height. In this paper, dry versions of the three parameterizations are employed to examine how the results compare with similarity theory, LES simulations and observations, and how they differ from each other. Some conclusions on possible inaccuracies and biases of the schemes are presented.

Momentum and thermodynamic equations are written as

$$\frac{\partial u}{\partial t} = f\,(v - V_g) - \frac{\partial}{\partial z}\langle u'w'\rangle \;, \tag{1a}$$

$$\frac{\partial v}{\partial t} = -f\,(u - U_g) - \frac{\partial}{\partial z}\langle v'w'\rangle \;, \tag{1b}$$

$$\frac{\partial \theta}{\partial t} = -\frac{\partial}{\partial z}\langle w'\theta'\rangle \;. \tag{1c}$$

Geostrophic wind (U_g, V_g) is prescribed. Roughness length is set to 0.2 m and $\ln(z_o/z_h) = 2$ (Garratt 1992), except for the MYJ scheme. Soil temperature varies sinusoidally over 24 hours with an amplitude of 10 K and is not affected by the atmosphere (Fig. 1). Divergences of fluxes $\partial\langle w'\phi'\rangle/\partial z$ are provided by the PBL schemes. The grid is stretched with a factor of about 1.1 from the first 'w' level about 20 m above the surface to 250 m at the 41st level at 5000 m. Equations are solved using the Crank–Nicholson scheme in 6-h integrations.

2. WRF IN THE SURFACE LAYER

Surface layer (SL hereafter) is the lowest part of the atmosphere, typically about a tenth of the height of the BL where surface fluxes of scalars and momentum, nearly constant with height in this layer, dominate dynamics and physics. Vertical profiles of scalars and wind are determined by the Monin-Obukhov similarity theory. Near the surface, BL parameterizations should give results which closely follow those prescribed by the theory i.e.:

$$\varphi - \varphi_0 = \frac{\varphi_*}{k}\left[\log\left(\frac{z}{z_\varphi}\right) - \Psi\left(\frac{z}{L}\right)\right] \;, \tag{2a}$$

where φ is any of u, v, θ_v, q, or other scalar, L is the M–O length defined by

$$L = \frac{u_*^2}{\left[k\,(g/\theta_v)\,\theta_{v*}\right]} \;, \tag{2b}$$

and function Ψ is given by Dyer (1974) for unstable conditions and Holtstag and De Bruin (1988) for stable conditions. Because of the complex form of function Ψ Eq. 2 is implicit and requires an iterative solution.

The MYJ scheme has its own procedure for matching the viscous sublayer and surface layer (Janjić 1994), while both MRF and YSU schemes calculate fluxes based on logarithmic similarity formulas. Instead of an iterative solution, MRF and YSU use approximations for Ψ. Figure 2 illustrates the differences between the iterative solution and results from the WRF approximation for surface drag coefficients (for convective conditions, regime 4 in WRF is plotted). The iterative solution is obtained with the Newton–Raphson algorithm, which rapidly converges and usually requires few iterations starting with the value from the previous time step. Possibly, the iterative solution is a viable alternative to the WRF approximation in light of the deficiencies of the latter as seen in the Fig. 2. It can be seen that for convective conditions for small roughness (e.g. over ocean) heat fluxes are underestimated and overestimated for high roughness (e.g. urban land).

Figure 3a shows potential temperature profiles from simulations for the three schemes in convective conditions integrated starting, at 6 local time and corresponding profiles calculated using similarity theory (near zero geostrophic wind assumed). The latter are obtained using the value of θ_* calculated by each scheme. It can be noted that the MYJ scheme fails to

*[In collaboration with the Cooperative Institute for Research in the Atmosphere (CIRA), Colorado State University, Fort Collins, Colorado] *Corresponding author address:* Dr. Mariusz Pagowski, email: Mariusz.Pagowski@noaa.gov

sufficiently transfer heat between the surface and the atmosphere, since the temperature difference between the atmosphere and the surface is several times larger than the corresponding value prescribed by the similarity. In both the MRF and YSU schemes heat transfer between the surface and the atmosphere is also underestimated but not as significantly as for MYJ. The MRF temperature profile seems to be lacking proper curvature in the SL as the scheme mixes the air above too strongly.

In the neutral conditions all of the schemes quite accurately follow logarithmic wind profiles prescribed by the similarity.

Potential temperature and wind profiles in stable conditions after integration starting at 18 local time with $(U_g, V_g) = (15, 0)$ are shown in Fig. 3b, c. Potential temperature profiles suggest that in the MYJ scheme the gradient between the atmosphere and the surface is too steep compared to the similarity, as was also the case for the convective BL. Also above the SL, the heat flux is insufficient for this scheme. The MRF fails to reproduce the curvature of the potential temperature profile, but instead it generates a log-linear profile with insufficient mixing. The MYJ and YSU schemes quite accurately model momentum transfer while the MRF does not account for profile curvature in these conditions.

It appears that in all stability conditions, MRF wind and potential temperature profiles follow equation

$$\varphi - \varphi_0 = \frac{\varphi_*}{k}\left[A \log\left(\frac{z}{z_\varphi}\right) + B\right] , \qquad (3)$$

where A and B are stability but not height dependent, rather than Eq. 2a. The MYJ scheme is clearly the most decoupled from the surface in terms of heat transfer, since temperature gradient between the surface and the atmosphere is too steep compared to the similarity.

3. WRF ABOVE THE SURFACE LAYER

The performance of the WRF BL schemes in convective conditions is illustrated in Fig. 4. Analysis of potential temperature profiles confirms conclusions from section 2 that the MYJ BL is much cooler than the other schemes. The depth of the BL for this scheme is about half of that for the MRF and YSU schemes. Both MRF and YSU produce similar stratification. In cases (not shown) where the geostrophic wind was increased, the BL was slightly deeper for MRF scheme (about 10% for $(U_g, V_g) = (15, 0)$). Analysis of heat flux in this figure shows that the explicit MYJ scheme might become numerically unstable for large values of diffusivities. In the analyzed cases this instability had marginal influence on potential temperature and wind. To obtain a smooth mixing, the time step needed to be decreased from 30 s to 2 s for this scheme. Observations and modeling consistently show that the virtual heat flux at the inversion level (entrainment flux) is about –0.2 of the surface heat flux value and about –0.3 for the dry flux when the contribution of mechanical turbulence is negligible. For the YSU scheme the prescribed entrainment flux matches that recommended value, while for the MRF scheme it is significantly below the expectation. The TKE-based 1.5-order MYJ scheme has near-zero entrainment flux since it is local and in the absence of shear, values of diffusivities are very small. This fact contributes to the slow BL growth in MYJ under these conditions.

WRF wind profiles in neutral conditions with $(U_g, V_g) = (10, 0))$ are shown in Fig. 5. Apparently, mixing is strongest when using the MRF scheme and weakest for the YSU scheme. Accordingly, the BL depth is enhanced by the MRF compared to the YSU. Wind turning, a consequence of the smallest v-stress divergence at the surface, with u-wind departures from geostrophy similar for all the schemes, is largest for YSU. In comparison with the LES, as well as with observations where negative $\langle u'w' \rangle$ flux is absent altogether, this scheme fares better than the other two.

The opposite holds true for stable conditions in Fig. 6, where mixing is strongest for the YSU scheme resulting in a deeper BL compared to the MRF and MYJ. In concert with considerations in section 2, potential temperature is lowest for the YSU scheme because of the increased wind stress for this scheme. In comparison with observations, it appears that the YSU heat flux is still too weak in the BL while stress is modeled quite accurately, and other schemes fare less favorably. In MYJ, which also develops an unexpected kink at the top of the BL, wind turning is strongest.

4. CONCLUSIONS

Comparison of bulk transfer coefficients for heat and momentum showed that approximations of similarity functions taken in the WRF might produce erroneous values of these coefficients. A proposition on iterative evaluation of the bulk transfer coefficients was suggested.

Behavior of the WRF in the SL when compared with similarity shows that all the schemes insufficiently transfer heat from/to the surface, suggesting that diurnal variation in the WRF SL, and consequently the whole BL, might be too weak or delayed, especially for the MYJ scheme. A lack of curvature in the MRF profiles suggests poor performance of this scheme in the SL.

Analysis of behavior of the WRF BL schemes above the SL confirms some of the deficiencies of the schemes in the SL, primarily insufficient heat transfer for the MYJ scheme. In the convective conditions with weak wind, the MRF and YSU develop a BL twice as deep as the MYJ. In stronger winds (not shown), the YSU produced a shallower BL, which might signal an improved performance in light of known overpredictions of the BL height by the MRF. The MYJ scheme became numerically unstable for large values of diffusivities in convective conditions. In neutral conditions mixing was least pronounced for the YSU scheme, with the opposite true for the stable BL.

Based on the results of idealized tests, it appears that the YSU scheme performs better than the MRF and MYJ under a variety of stability conditions when compared with theory, LES simulations, and a limited number of observations. Nevertheless, the conclusions derived from these tests cannot substitute for extensive verification of the schemes in daily forecasts evaluated against a broad range of measurements.

5. REFERENCES

Dyer, A.J., 1974: A review of flux-profile relationships, *Boundary-Layer Meteorol.*, **7**, 363-372.

Garratt, J.R., 1992: The atmospheric boundary layer, Cambridge University Press, 316 pp..

Holtslag, A.A.M. and De Bruin, H.A.R., 1988: Applied modeling of the night-time surface energy balance over land, *J. Appl. Meteor.*, **27**, 689–704.

Hong, S.-Y, and J. Dudhia, 2003: Testing of a new non-local boundary layer vertical diffusion scheme in numerical weather prediction applications, 20th Conference on Weather Analysis and Forecasting/16th Conference on Numerical Weather Prediction, Seattle, WA.

Hong, S.-Y, and H.-L. Pan, 1996: Non-local boundary layer vertical diffusion in Medium-Range Forecast model, *Mon. Wea. Rev.*, **124**, 1215–1238.

Janjic, Z.I., 1994: The step-mountain eta coordinate model: further developments of the convection, viscous layer, and turbulence closure schemes, *Mon. Wea. Rev.*, **122**, 927–945.

Mason, P.J., and D.J. Thomson, 1987: Large-eddy simulations of the neutral-static-stability planetary boundary layer, *Quart. J. Roy. Meteor. Soc.*, **113**, 413–443.

Mellor, G.L., and T. Yamada, 1982: Development of turbulence closure model for geophysical fluid problems, *Rev. Geophys. Space Phys.*, **20**, 851–875.

Nicholls, S., 1985: Aircraft observations of the Ekman layer during the joint air-sea interaction experiment, *Quart. J. Roy. Meteor. Soc.*, **111**, 391–426.

Nieuwstadt, F.T.M., 1985: A model of the stationary, stable boundary layer, in *Turbulence and Diffusion in Stable Environments*, ed. J.C.R. Hunt, pp. 149–79.

Stull, R.B., 1988: An introduction to boundary layer meteorology, Kluwer Academic Publishers, 666 pp.

Troen, I., and L. Mahrt, 1986: Simple model of the atmospheric boundary layer; sensitivity to surface evaporation, *Boundary-Layer Meteorol.*, **37**, 129–148.

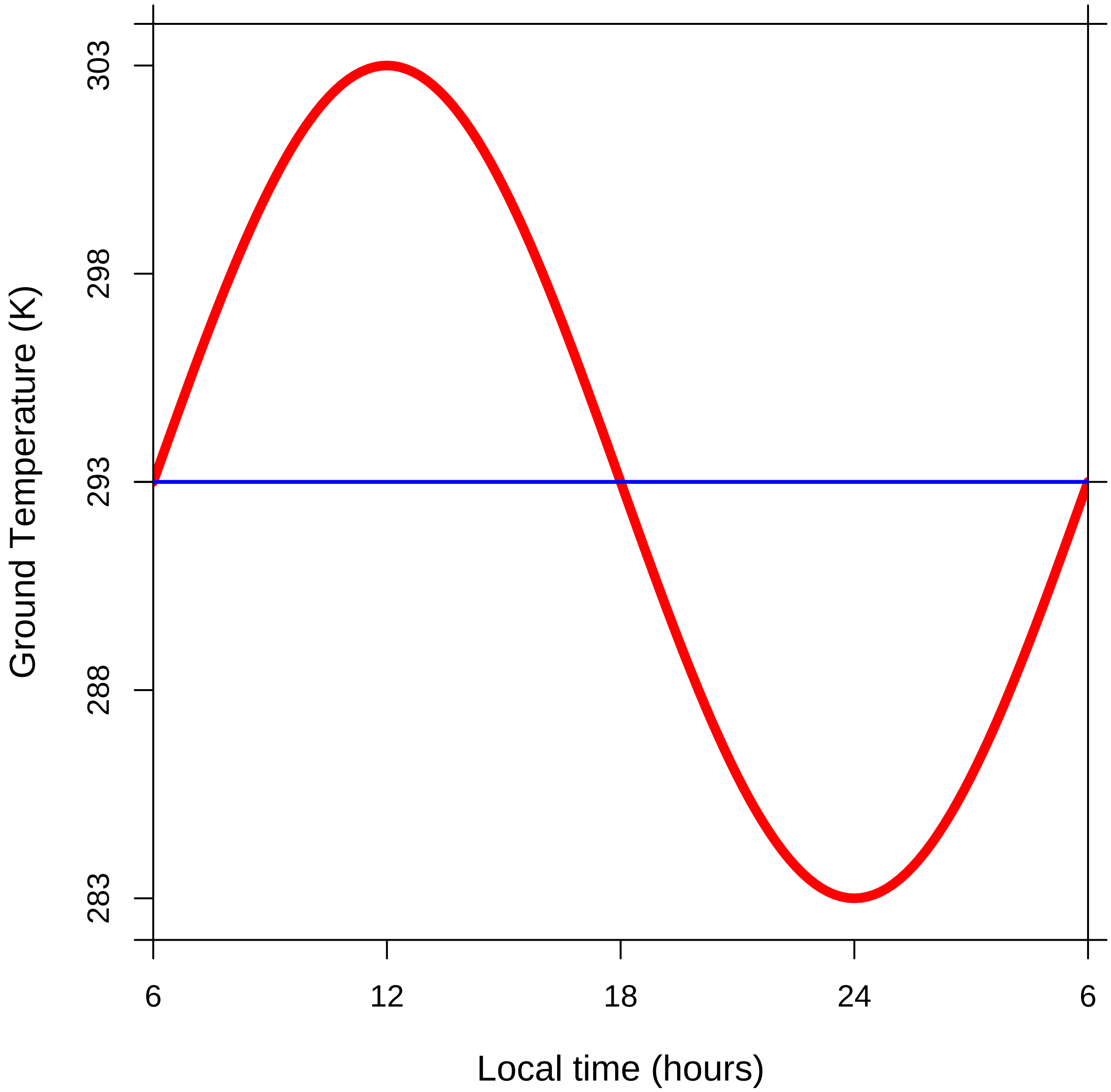

Figure 1: Temporal variation of surface temperature.

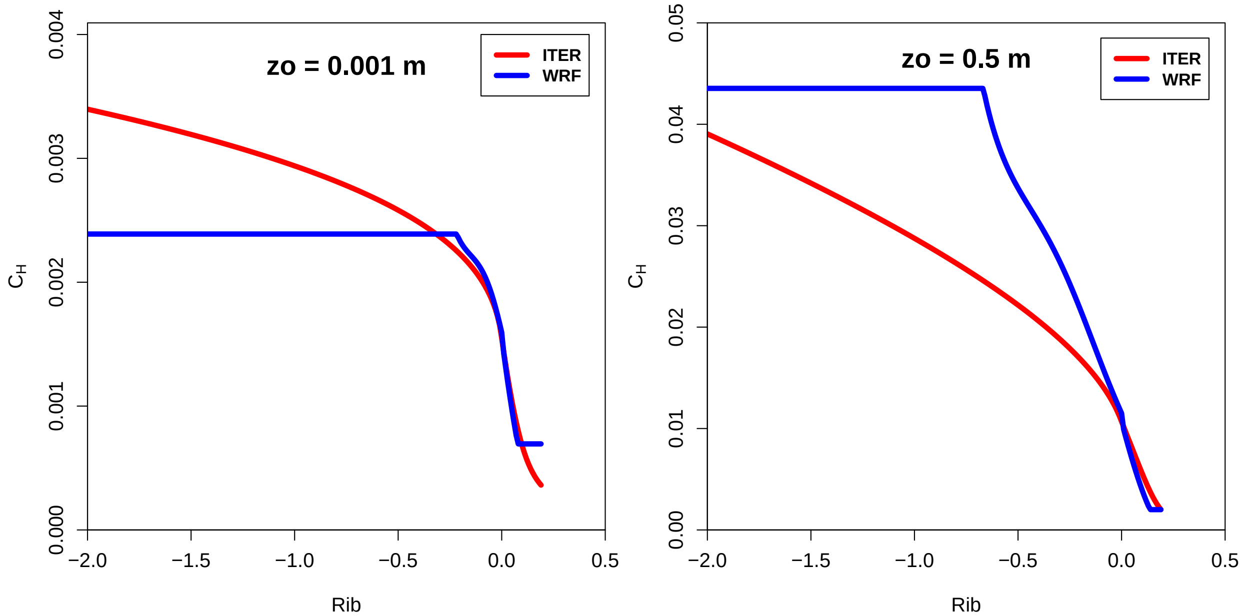

Figure 2: Heat transfer coefficients vs. bulk Richardson number obtained iteratively and using the WRF approximation for two values of surface roughness.

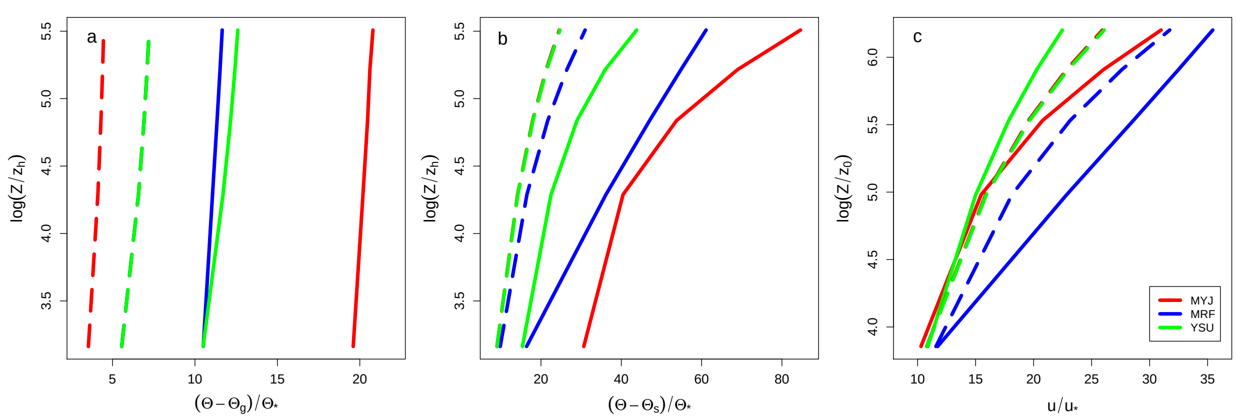

Figure 3: Profiles of potential temperature (a,b) and velocity (c) for the MYJ, MRF and YSU schemes in the surface layer in convective (a) and stable (b,c) conditions. YSU overlays MRF in (a). YSU overlays MYJ in (b). Dashed lines denote profiles obtained using similarity.

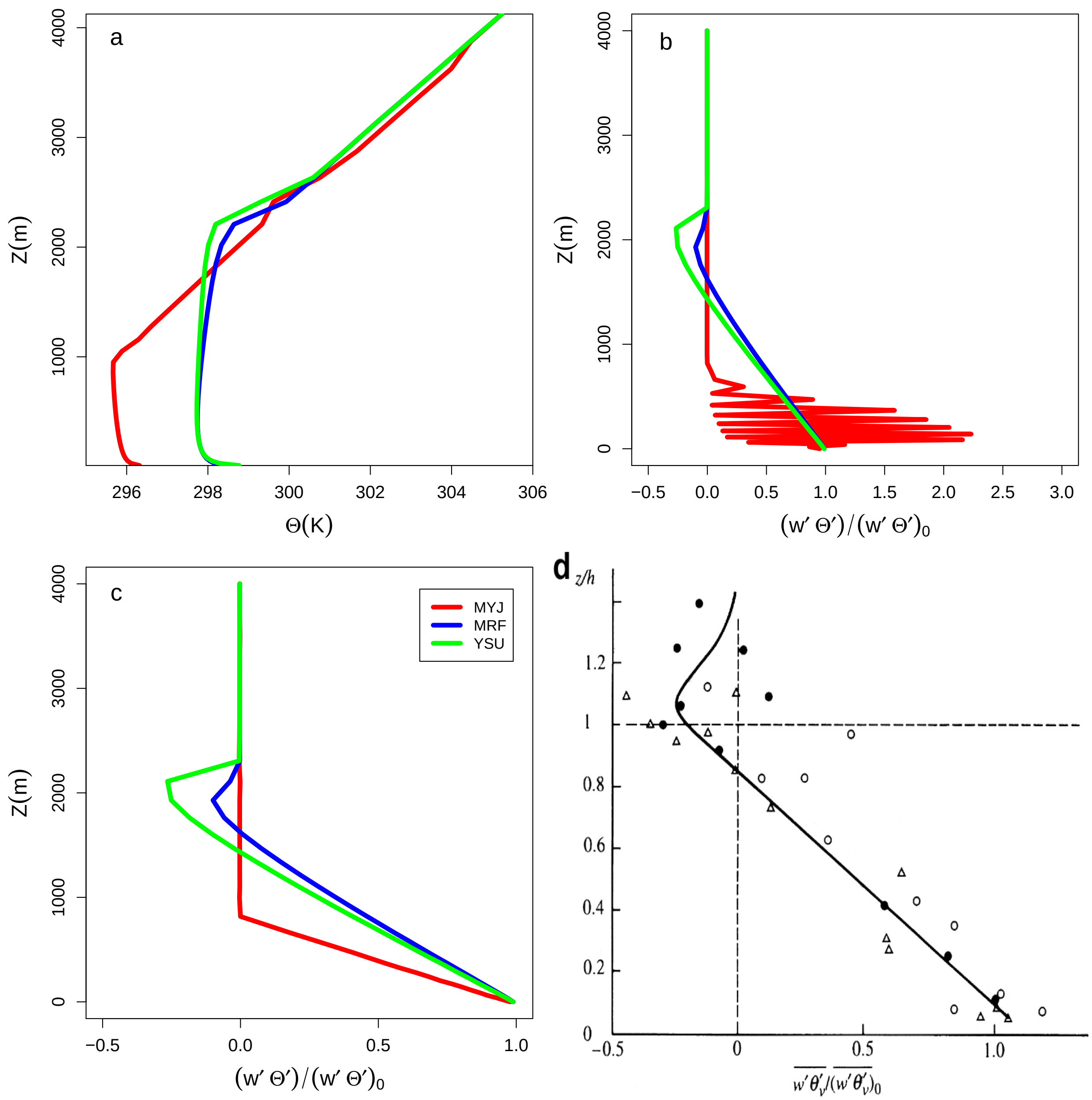

Figure 4: Profiles of potential temperature (a), heat flux with 30 s time step (b) and 2 s time step (c) for the MYJ, MRF and YSU schemes in convective conditions and observations (d) (from Garratt 1992, Fig. 6.2 based on Stull 1988).

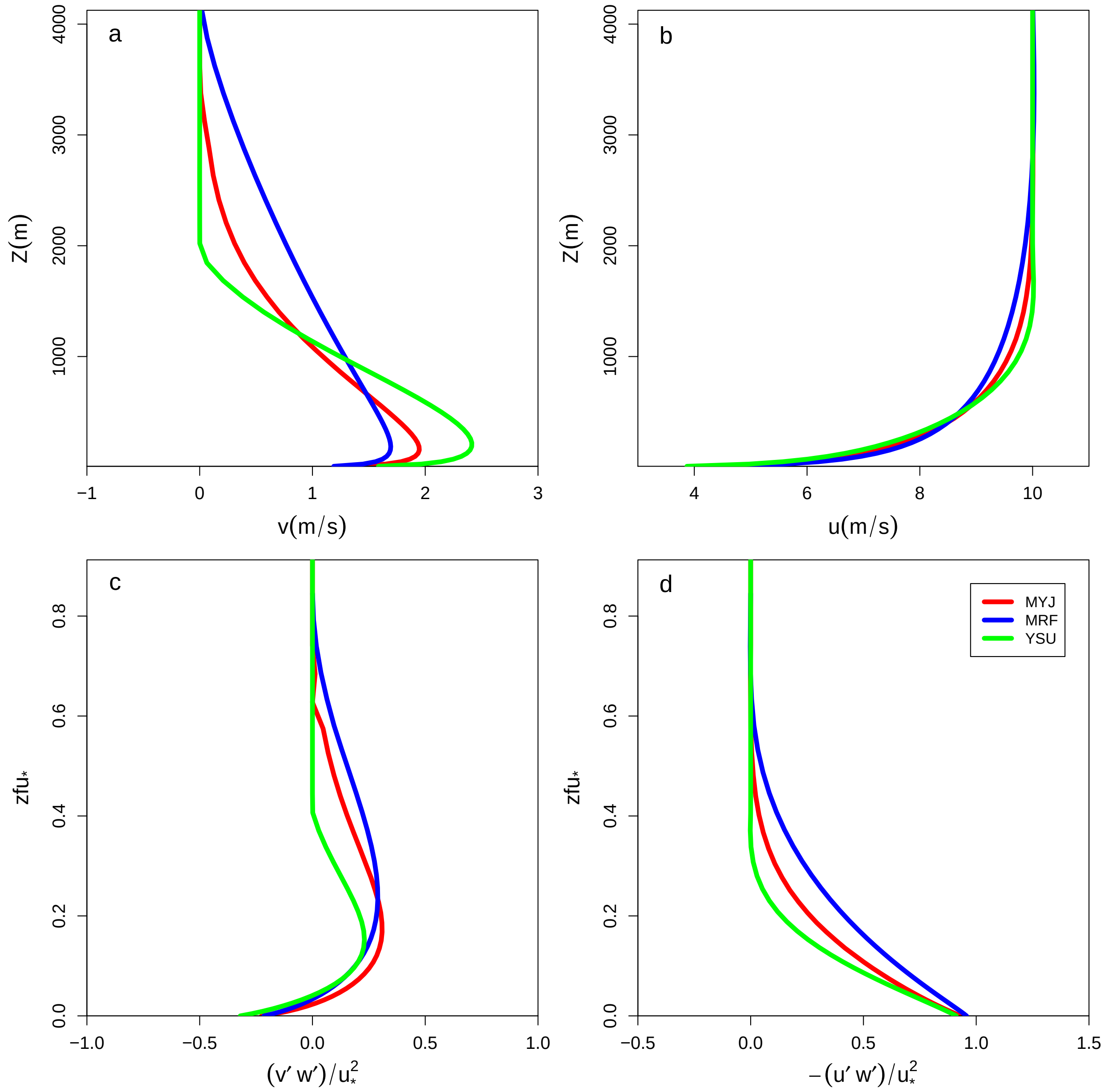

Figure 5: Profiles of wind: v (a), u (b), stresses: $\langle v'w' \rangle$ (c), $\langle u'w' \rangle$ (d) for the MYJ, MRF and YSU schemes in neutral conditions, observations and LES results (e) (from Garratt, Fig. 3.3, based on Nicholls 1985 and Mason and Thomson 1987).

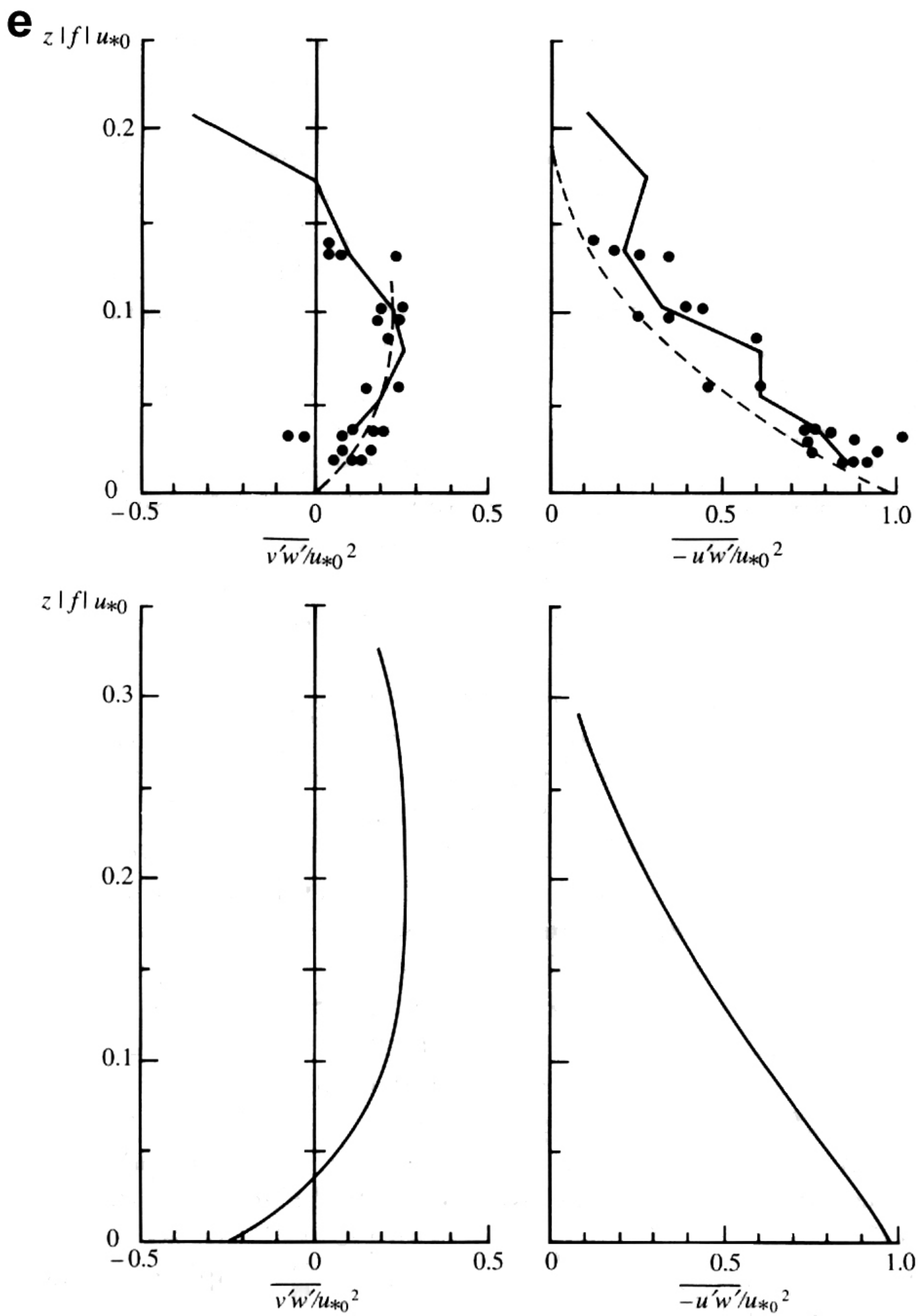
e
z | f | u*0
0.2
0.1
0
−0.5
0
0.5
v′w′/u*0²
0
0.5
1.0
−u′w′/u*0²
z | f | u*0
0.3
0.2
0.1
0
−0.5
0
0.5
v′w′/u*0²
0
0.5
1.0
−u′w′/u*0²

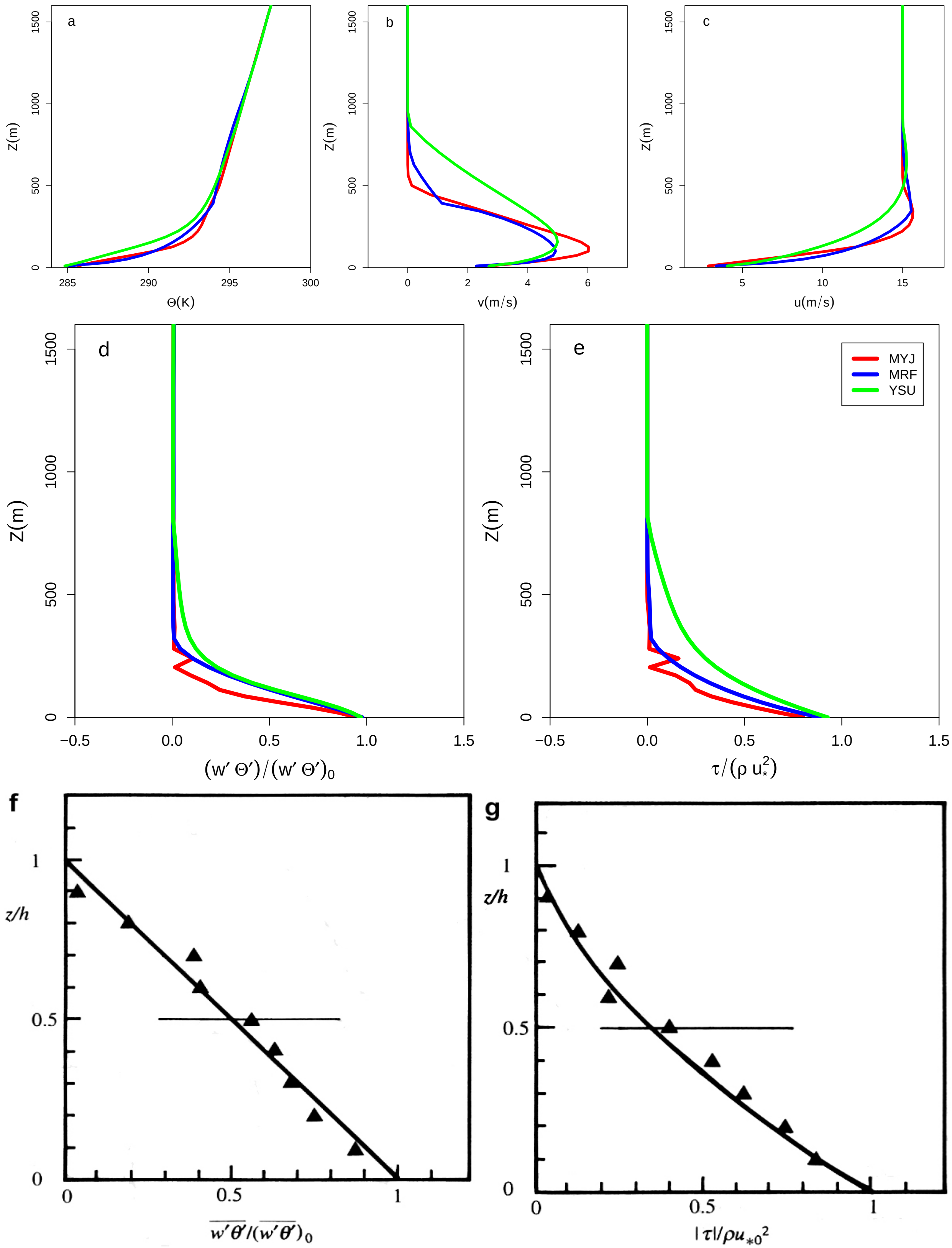

Figure 6: Profiles of potential temperature (a) , wind: v (b), u (c), heat flux (d), total stress (e) for the MYJ, MRF and YSU schemes in stable conditions, observations: heat flux (f) and total stress (g) (from Nieuwstadt 1985).